FAD-SPADs: a New Paradigm for Designing Single-Photon Detecting Arrays

Mel White[1†], Tianyi Zhang[1†], Akshat Dave[1], Shahaboddin Ghajari[2], Alyosha Molnar[2], and Ashok Veeraraghavan[1]

[†]Indicates equal contribution
[1]Rice University, Houston, TX
[2]Cornell University, Ithaca, NY

***Abstract*—We present a novel architecture for the design of single-photon detecting arrays that captures relative intensity or timing information from a scene, rather than absolute. The proposed method for capturing relative information between pixels or groups of pixels requires very little circuitry, and thus allows for a significantly higher pixel packing factor than is possible with per-pixel TDC approaches. The inherently compressive nature of the differential measurements also reduces data throughput and lends itself to physical implementations of compressed sensing, such as Haar wavelets. We demonstrate this technique for HDR imaging and LiDAR, and describe possible future applications.**

***Index Terms*—SPAD, LiDAR, HDR, compressed sensing, computational imaging**

I. Introduction

Single-Photon Avalanche Diodes (SPADs) are highly sensitive photodiodes which can detect individual photons with extremely fast response and high precision. For this reason, they have become the gold standard in many photon-limited imaging applications [1], [2]. However, current SPAD array designs suffer from low spatial resolution due to complex circuitry and high data throughput needed for capturing absolute timestamps or photon counting, which limits their usage in many downstream applications. We present a novel, lightweight readout architecture which overcomes existing challenges in SPAD array designs: first arrival differential SPADs (FAD-SPADs). Our technique differs from previously proposed hardware solutions such as Time to Digital Converter (TDC) sharing, adaptive sensing [3], data sketching [4], and sensor fusion [5], [6] because it is not TDC-based, and instead relies on small circuits that perform data compression at the sensor.

FAD-SPADs record differential measurements between pixels, either in intensity or time of flight. Our key insight is that rich information is encoded in the relative timing of the first photon captured within a time window (See Fig. IV), and this information can be captured by small and simple digital circuitry. This method can also provide gains in certain imaging metrics, including significantly reduced circuit footprint and better pixel packing, orders of magnitude data size reduction, and improved dynamic range.

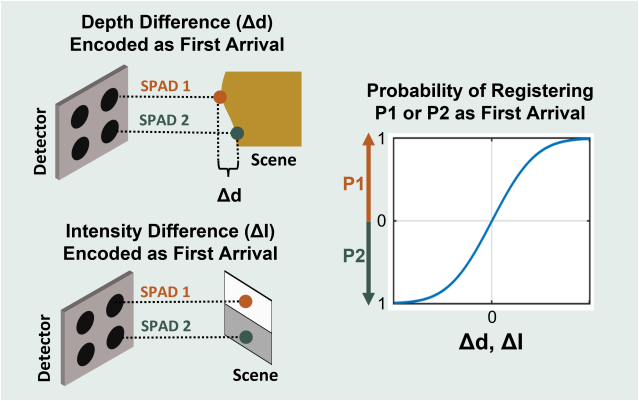

Fig. 1. FAD-SPAD operation principle. 1: Either depth intensity differences can be encoded with the first arrival of a photon within a time window. 2: The relationship between the relative flux and the probability of recording an up or down count with digital circuitry is nonlinear.

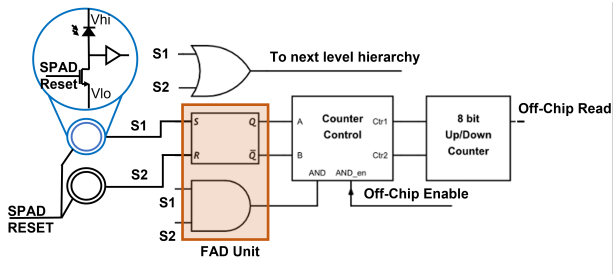

Fig. 2. FAD-SPAD readout circuitry. The SPADs are grouped, and each group is connected to the SR-Latch. Based on which group detects a photon first the counter will count up or down.

II. Key Concept: the FAD unit

Let us first consider the case of only two SPAD pixels. We connect their readout to the inputs of an SR latch, as shown in Fig. 2. The first photon event on either of the two pixels triggers the latch, which holds its state regardless of subsequent photon events on either pixel. This information is passed to an up/down counter, which counts up if pixel 1 saw the first event, down if pixel 2 saw the first event, and holds its state if no events were detected. After a short time window (T), the latch and SPADs are reset to the "listening" state, and this process is repeated for N cycles. With the counter

Mel White is the corresponding author and can be reached at:
email: mel.white@rice.edu.

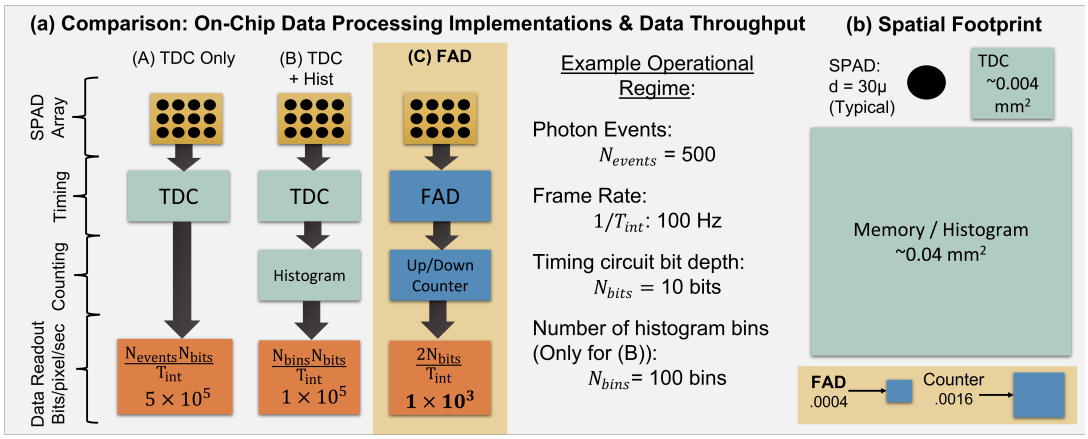

Fig. 3. A comparison of the estimated data throughput and circuit footprint for conventional approaches compared to ours (in highlighted gold boxes). At the operating conditions given in the figure, our data throughput is two orders of magnitude smaller while only using only 5% of the circuit footprint.

initialized to a midpoint, the resulting readout from the counter measures the relative flux between the two pixels. An OR gate connected to both SPADs allows us to pass this information along to other groups of pixels, or even a cumulative output. With the addition of an optionally-enabled AND gate, we can further distinguish between dual events (where both SPADs see a photon) and single events (only one SPAD sees a photon).

These circuits are extremely compact and throughput-efficient (see Fig. 3 for details) and thus scalable to large arrays. Critically, only the FAD unit need be placed inside the array and near the actual SPADs for accuracy; the counter and other supporting circuitry can be outside of the array, and do not impact the fill factor or spatial resolution. The FAD unit can be constructed of only 12 transistors: 8 for a NAND-type SR latch, and 4 for the AND gate. We contrast this to the use of per-pixel TDCs, which are often 3x-4x larger than the SPAD itself, and must be placed immediately adjacent to the pixel for accurate measurements.

A. Relationship between differential flux and counter readout

Uncertainty from photon noise provides a nonlinear relationship between the relative fluxes at each pixel and the recorded count. This relationship is expressed mathematically as the difference between the probability of an up or down count times the number of cycles. Taking the fluxes at the two SPADs to be Φ_1 and Φ_2 (photon flux per cycle), and assuming Poisson arrival processes at both SPADs, this gives:

$$\mathbb{E}(\mathbb{D}) = N_{cycles}[1 - e^{-(\Phi_1+\Phi_2)T}]\left(\frac{\Phi_1 - \Phi_2}{\Phi_1 + \Phi_2}\right) \quad (1)$$

Where T is the period of the detection cycle.

B. Connectivity schemes

To build upon the core concept described for two SPADs, pixels can be grouped together via OR gates at their output. Thus, if the first photon hits any pixel in group A before group B, the SR latch will count up, and vice versa for group B. Moreover, SPADs may be connected to many different groups simultaneously, allowing for simultaneous differential measurements.

Some possible configurations are shown in Fig. 4. Local groupings will suppress local background, while other kinds of clustering mimicking Haar or Hadamard transforms enable data compression at the sensor.

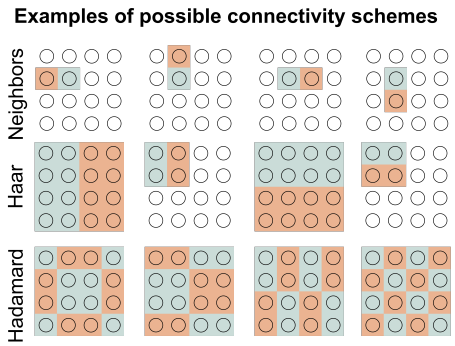

Fig. 4. Some examples of 'OR' connected groups in a 4×4 array. The choice of grouping will impact the data bandwidth and SNR of the reconstructed image.

III. Encoding First Arrival as Intensity Difference

In a passive lighting arrangement, the differential information reflects the intensity of the scene. A SPAD saturates if it detects one photon, and so it may seem counter-intuitive to use them in high dynamic range imaging applications. Yet, several recent works [7], [8] have shown that single-photon sensitivity and non-linear behavior of SPADs can be exploited for high dynamic range imaging. The major drawback of existing SPAD array architectures is that they suffer from limited photon counter bit depth; under high photon flux, the individual photon counters saturate, and any local differences in intensity are lost. Our approach uses relative rather than absolute timing information, which will not saturate under small local gradients, as illustrated in Fig. 5. This can also be inferred from Equation 1. As fluxes Φ_1 and Φ_2 increase, the exponential term disappears, but the differential term in the numerator remains. As long as the difference does not

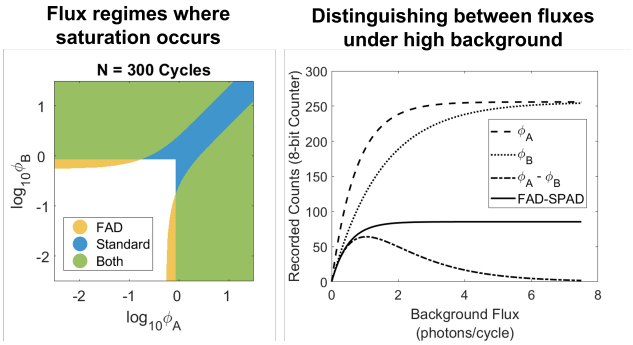

Fig. 5. Left: when the fluxes at pixels A and B are both high, regular counters will saturate, but the FAD does not. Right: under high background lighting conditions, the difference between SPADs with counters vanishes; FAD-SPADs preserve the difference.

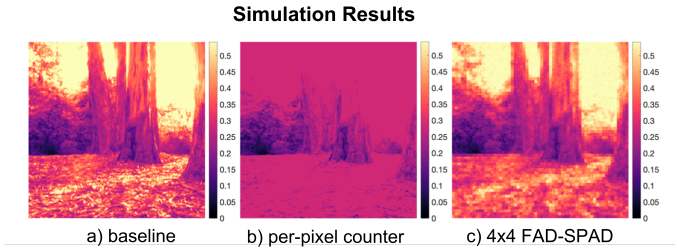

Fig. 6. A simulation showing how FAD-SPADs preserve high dynamic range of an image. The "blocky" artifacts in our result are due to the fact that we simulated a scanning 4x4 array (to mimic our prototype).

exceed the limits of the counter, the difference is preserved, theoretically, under infinite background flux. Fig.6 illustrates how small flux differences are preserved, even under high-flux background conditions. The dynamic range of FAD-SPADs is in practice determined by the largest and smallest detectable signal, limited by SNR. The interesting case is under high flux conditions (at low flux, it behaves exactly as two independent SPADs).

To show that this can be practically achieved, we have implemented a proof-of-concept prototype containing 16 pixels (4x4) using a conventional 180 nm CMOS process with a Haar grouping scheme, shown in Fig. 7 [9]. While this implementation includes only two layers of hierarchy of Haar wavelets, the small size of the local digital circuitry means this design is scalable to any $2^N \times 2^N$ array. Notably, the Haar pixel grouping scheme combined with the compact size of the support circuitry results in minimal impact on device's footprint; with no additional design effort, we achieve a 34% fill factor.

IV. Encoding First Arrival as Depth Difference

Flash LiDAR systems utilize SPAD arrays to perform single-shot 3D imaging without the need for mechanical scanning [10]. However, SPAD arrays require per-pixel timing circuits (TDCs) with high spatial footprint and data throughput limiting the spatial and temporal resolution of such systems. In contrast to TDCs, the FAD units are more lightweight and are capable of depth difference between pairs of pixels.

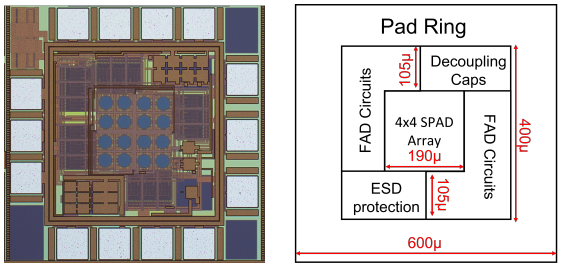

Fig. 7. A micrograph of the fabricated prototype in 180 nm CMOS. The 4x4 array (excluding the pad ring and supporting circuitry) measures $190\mu m \times 190\mu m$ and has a fill factor of 34%.

Using the FAD units, we design a flash LiDAR system that can perform high-resolution 3D imaging and scene inference [11]. The core idea is that FAD captures the relative order of photon arrivals at the two pixels. There exists a one-to-one mapping between this differential measurement and depth differences between the two pixels. FAD-LiDAR enables 3D inference tasks, including depth edge detection, depth-based segmentation, surface normal estimation, and depth imaging with only a few TDCs as shown in Fig. 8. It is worth noting that for cases where absolute depth is not required, our approach can be implemented without any TDCs.

Consider that the laser and detector are collocated. Assume SPAD pixel 1 points to a scene location that is closer to the detector, and SPAD pixel 2 to a farther location (in a setup shown in the bottom left section of Fig.). Then, within a time window, photons reaching SPAD pixel 1 are more likely to arrive earlier than photons from SPAD pixel 2. Over a large number of cycles, the relative frequency of first arrival photons between the pixels can capture information about depth difference Δd. This leads to a monotonic mapping between the FAD measurements, FAD, and the depth difference, $\Delta\tau$, as

$$FAD \propto -N_{\text{cycles}}\alpha_1\alpha_2\left(\frac{\Delta\tau}{2\sigma}\right) \tag{2}$$

where N_{cycles} is the total number of laser cycles and α_1, α_2 are the photon flux (per cycle) at the two pixel locations 1 and 2. We can acquire intensity estimates $\hat{\alpha_1}$, $\hat{\alpha_2}$ by using intensity measurements. To decouple illumination effects caused by single photon arrivals, we (1) enable the AND gate so that only when both pixels receive returning photons does FAD perform a comparison (2) measure intensity values at each pixel and factor them out. After these operations, we reach a normalized FAD measurement $nFAD$ that is only dependent on the relative depth between two pixels.

$$nFAD = \frac{FAD}{N_{\text{cycles}}\hat{\alpha_1}\hat{\alpha_2}} \tag{3}$$

$$nFAD \propto -\left(\frac{\Delta\tau}{2\sigma}\right) \tag{4}$$

Using FAD units and nearest-neighbor connectivity, we directly perform 3D scene inference tasks as shown in (Fig. 8). Tasks such as depth edge detection, depth-based segmentation, and normal estimation are sufficient with FAD measurements

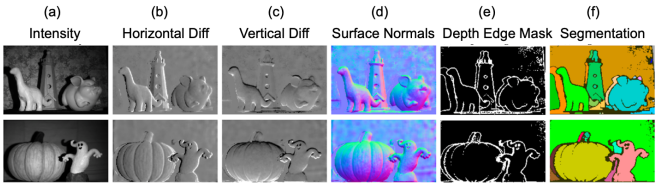

Fig. 8. 3D imaging applications of FAD LiDAR. Column (a): intensity view of the scenes. Columns (b) to (f) correspond to different 3D applications as labeled in the figure.

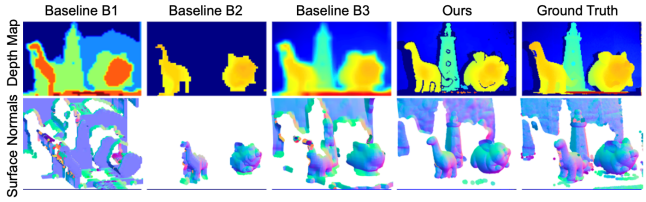

Fig. 9. High-resolution 3D imaging and surface normals by FAD LiDAR emulated using a single-pixel SPAD setup. Reconstruction from a scanning-based LiDAR design is denoted as Ground Truth. Conventional flash LiDAR designs B1, B2, and B3 (see [11] for details) suffer from performance tradeoffs resulting in poor depth resolution (B1), range (B2), or spatial resolution (B3). Our differential flash design offers significantly better reconstruction quality for the same data throughput as conventional baselines.

(relative depth information) and per-pixel intensity estimates. Depth edge detection and segmentation can be performed by appropriately thresholding nFAD measurements, while normal estimation requires a two-step procedure: first inverting relative depth difference from nFAD, then performing Poisson integration [12] to generate clean surface normal estimates.

To reconstruct absolute depth across the scene, we can capture a few absolute ToF measurements by sparsely distributing TDCs across the FAD array. We show that FAD-based LiDAR provides depth maps at higher resolution and range than existing TDC-based flash LiDAR, and demonstrate via emulation that FAD-LiDAR provides improved performance for the same data bandwidth (Fig. 9).

V. Conclusions and Discussion of Future Directions

In this paper we present techniques and supporting analysis for a novel type of SPAD array design based on differential sensing. We also present two applications: HDR imaging and 3D imaging, featuring two architectures (Haar and nearest neighbor). However, this is only a small sample of the capabilities enabled by FAD architectures.

For example, the differential nature of FAD units is inherently amplifying of local differences and thus could enhance contrast in bioimaging applications, such as the loss in contrast due to scattering.

There is also fertile space for analysis of other differential connectivity schemes to enable compressed sensing of images. Binary compressed sensing matrices (eg, Hadamard transforms) can be implemented similarly to our Haar example for HDR by simply changing the connected groups. The differential grouped measurements could also be used to do adaptive sensing in sparse image acquisition. For example, if a large differential signal is found in one region of an image, then a smart sensor could continue to collect finer-grained measurements in that region, and not collect redundant data in a region of the image that lacks contrast.

Finally, the gains in circuit footprint and scalability of the concept we show here could facilitate the development of larger and denser SPAD arrays with high photon detection probability.

References

[1] C. Bruschini, H. Homulle, I. M. Antolovic, S. Burri, and E. Charbon, "Single-photon avalanche diode imagers in biophotonics: review and outlook." *Light: Science & Applications*, vol. 8, no. 87, 2019.

[2] F. Villa, F. Severini, F. Madonini, and F. Zappa, "SPADs and SiPMs arrays for long-range high-speed light detection and ranging (LiDAR)," *Sensors*, vol. 21, no. 11, 2021.

[3] C. Zhang, S. Lindner, I. M. Antolović, J. M. Pavia, M. Wolf, and E. Charbon, "A 30-frames/s, 252×144 SPAD flash LiDAR with 1728 dual-clock 48.8-ps TDCs, and pixel-wise integrated histogramming," *IEEE Journal of Solid-State Circuits*, vol. 54, no. 4, pp. 1137–1151, 2018.

[4] M. P. Sheehan, J. Tachella, and M. E. Davies, "A sketching framework for reduced data transfer in photon counting LiDAR," *IEEE Transactions on Computational Imaging*, vol. 7, pp. 989–1004, 2021.

[5] D. B. Lindell, M. O'Toole, and G. Wetzstein, "Single-photon 3D imaging with deep sensor fusion." *ACM Trans. Graph.*, vol. 37, no. 4, pp. 113–1, 2018.

[6] Y. Liu, F. Gutierrez-Barragan, A. Ingle, M. Gupta, and A. Velten, "Single-photon camera guided extreme dynamic range imaging," in *Proceedings of the IEEE/CVF Winter Conference on Applications of Computer Vision*, 2022, pp. 1575–1585.

[7] A. Ingle, A. Velten, and M. Gupta, "High flux passive imaging with single-photon sensors," in *Proceedings of the IEEE/CVF Conference on Computer Vision and Pattern Recognition*, 2019, pp. 6760–6769.

[8] M. Zarghami, L. Gasparini, M. Perenzoni, and L. Pancheri, "High dynamic range imaging with TDC-based CMOS SPAD arrays," *Instruments*, vol. 3, p. 38, 08 2019.

[9] M. White, S. Ghajari, T. Zhang, A. Dave, A. Veeraraghavan, and A. Molnar, "A differential SPAD array architecture in 0.18 μm CMOS for HDR imaging," in *2022 IEEE International Symposium on Circuits and Systems (ISCAS)*, 2022, pp. 292–296.

[10] F. Villa, F. Severini, F. Madonini, and F. Zappa, "Spads and sipms arrays for long-range high-speed light detection and ranging (lidar)," *Sensors*, vol. 21, no. 11, p. 3839, 2021.

[11] T. Zhang, M. J. White, A. Dave, S. Ghajari, A. Raghuram, A. C. Molnar, and A. Veeraraghavan, "First arrival differential LiDAR," in *2022 IEEE International Conference on Computational Photography (ICCP)*, 2022, pp. 1–12.

[12] R. T. Frankot and R. Chellappa, "A method for enforcing integrability in shape from shading algorithms," *IEEE Transactions on pattern analysis and machine intelligence*, vol. 10, no. 4, pp. 439–451, 1988.